International Journal of Innovation and Scientific Research
ISSN 2351-8014 Vol. 21 No. 2 Apr. 2016, pp. 367-375

http://www.ijisr.issr-journals.org/

Natural Convection Heat Transfer of the nanofluids in a Square Enclosure with an Inside Cold Obstacle

Zoubair Boulahia, Abderrahim Wakif, and Rachid Sehaqui

Hassan II University, Faculty of Sciences Aïn Chock, Laboratory of Mechanics,
BP 5366 Maarif, Casablanca, Morocco

ABSTRACT: This article presents a numerical study on natural convection heat transfer of nanofluid (Cu-water) in a square enclosure having a cold obstacle. The transport equations were solved using the finite difference formulation based on Alternating Direction Implicit method (ADI method). The method used is validated against previous works. Effects of various design parameters such as the height of the obstacle $(0.125 \leq H \leq 0.5)$, Rayleigh number $(10^3 \leq Ra \leq 10^6)$, and nanoparticles volume fraction $(0 \leq \varphi \leq 0.2)$ on the heat transfer are investigated. The results show that the heat transfer rate inside the enclosure increases by increasing the height of the cold block, the volume fraction of nanoparticles and Rayleigh number.

KEYWORDS: Enclosure, Natural Convection, Cooler, Nanofluid.

1 INTRODUCTION

For many years, natural convection and heat transfer in the square enclosures are encountered in a wide range of engineering applications, such as heating and cooling nuclear systems of reactors, lubrication technologies, cooling of electronic devices, ventilation of rooms with radiators, cooling of containers and heat exchangers. There are many studies concerning the heat transfer in rectangular or square cavities have been studied extensively in the literature. One of the first works on the numerical simulation of natural convection inside cavities is the pioneering work of De Vahl Davis [1]. He performed a numerical simulation on a square cavity with two vertical isothermal walls, one cold and one hot, and two horizontal adiabatic walls. This cavity with those boundary conditions is known as differentially heated cavity (DHC). AlAmiri et al [2] reported natural convection heat transfer in a partially divided square enclosure. The results showed that the heat transfer increases by increasing the height of block and volume fraction of the nanoparticles. The same problem was examined by Guiet et al [3] and Varol et al [4] in the case of a triangular enclosure. Boulahia and Sehaqui [5] investigated a numerical simulation of natural convection of nanofluid in a square cavity having a centrally square heater. Their simulations indicate that increasing the size of the heated block, and Rayleigh number leads to an increase in average Nusselt number. Bouafia and Daube [6] studied natural convection in cavity filled with air having a heated solid body. They observed that the induced disturbances determined for weakly supercritical regimes indicate the existence of two instability types driven by different physical mechanisms: shear and buoyancy-driven instabilities, according to whether the flow develops in a square or in a tall cavity. Ha and Jung [7] considered a numerical study on three dimensional conjugate heat transfer of natural convection and conduction in a differentially heated cubic enclosure having an internal heated square partition. They investigated the effects of three-dimensionalities on the fluid flow and thermal characteristics in the enclosure. Other studies were carried out on the natural convection of the nanofluid, for example, [8-9].

The objective of this work is to investigate the effects of volume fraction, the height of the cold block and Rayleigh number on the heat transfer of nanofluid (Cu-water) for natural convection in a square enclosure having a cold block. Our numerical results are presented in the form of plots of isotherms, streamlines and average Nusselt numbers to show the influence of nanofluid and the height of the cold block.

2 PROBLEM STATEMENT

The studied configuration and coordinate system of the considered enclosure in the present study are shown in Fig. 1. It is a differentially heated enclosure with an inside cold block, filled with nanofluids. The cold obstacle is maintained at a temperature T_c . The vertical walls are maintained respectively at hot (T_h) and cold (T_c) temperatures, the horizontal walls are adiabatic. It is assumed that the nanofluid is newtonian, incompressible and laminar. The base fluid and the nanoparticles are in a thermal equilibrium state. The thermo-physical properties of the nanofluid used in this study as listed in Table 1.

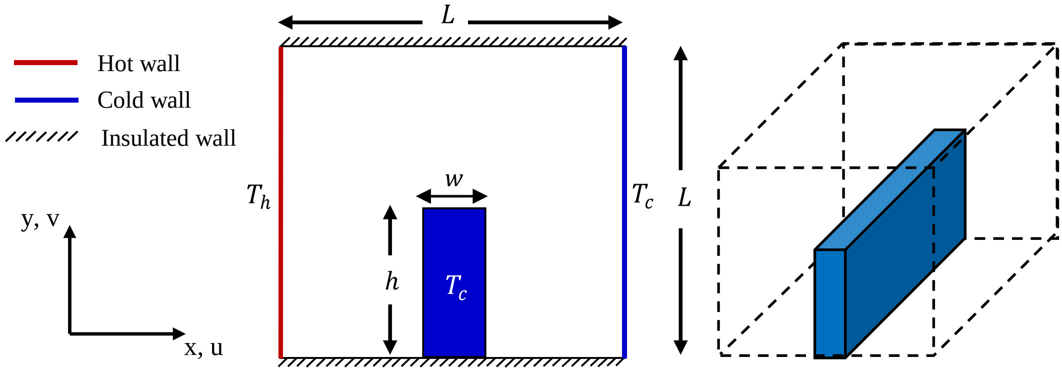

Fig. 1. Geometrical configuration and boundary conditions

Table 1. Thermo-physical properties of water and nanoparticles at T = 298 K

	Copper (Cu)	Water (H_2O) (25°C)
C_p(J/Kg K)	385	4179
ρ(Kg/m^3)	8933	997.1
k(W/mK)	401	0.6
β(K^{-1})	1.67 10^{-5}	2.1 10^{-4}
μ(kg m^{-1} s^{-1})	–	1.005 10^{-3}

3 MATHEMATICAL FORMULATION

The governing equations including the transient equations of the continuity, momentum and energy in terms of the stream–vorticity formulation for an incompressible flow are expressed in the following format:

$$\frac{\partial^2\tilde{\psi}}{\partial\tilde{x}^2}+\frac{\partial^2\tilde{\psi}}{\partial\tilde{y}^2}=-\tilde{\omega} \tag{1}$$

$$\frac{\partial\tilde{\omega}}{\partial\tilde{t}}+\frac{\partial\tilde{\psi}}{\partial\tilde{y}}\left(\frac{\partial\tilde{\omega}}{\partial\tilde{x}}\right)-\frac{\partial\tilde{\psi}}{\partial\tilde{x}}\left(\frac{\partial\tilde{\omega}}{\partial\tilde{y}}\right)=\nu_{nf}\left(\frac{\partial^2\tilde{\omega}}{\partial\tilde{x}^2}+\frac{\partial^2\tilde{\omega}}{\partial\tilde{y}^2}\right)+\frac{(\rho\beta)_{nf}}{\rho_{nf}}g\,\frac{\partial T}{\partial\tilde{x}} \tag{2}$$

$$\frac{\partial T}{\partial\tilde{t}}+\frac{\partial\tilde{\psi}}{\partial\tilde{y}}\left(\frac{\partial T}{\partial\tilde{x}}\right)-\frac{\partial\tilde{\psi}}{\partial\tilde{x}}\left(\frac{\partial T}{\partial\tilde{y}}\right)=\alpha_{nf}\left(\frac{\partial^2 T}{\partial\tilde{x}^2}+\frac{\partial^2 T}{\partial\tilde{y}^2}\right) \tag{3}$$

The horizontal and vertical velocities are given by the following relations:

$$\tilde{u}=\frac{\partial\tilde{\psi}}{\partial\tilde{y}},\quad \tilde{v}=-\frac{\partial\tilde{\psi}}{\partial\tilde{x}} \tag{4}$$

Where the nanofluid effective density, heat capacity, thermal expansion coefficient and thermal diffusivity are calculated from the following equations [10]:

$$\rho_{nf}=(1-\varphi)\rho_f+\varphi\rho_s \tag{5}$$

$$(\rho C_p)_{nf} = (1-\varphi)(\rho C_p)_f + \varphi(\rho C_p)_s \tag{6}$$

$$(\rho\beta)_{nf} = (1-\varphi)(\rho\beta)_f + \varphi(\rho\beta)_s \tag{7}$$

$$\alpha_{nf} = k_{nf}/(\rho C_p)_{nf} \tag{8}$$

The effective thermal conductivity of the nanofluid is approximated by the Maxwell–Garnetts (MG) model [15].

$$\frac{k_{nf}}{k_f} = \frac{k_s + 2k_f - 2(k_f - k_s)\varphi}{k_s + 2k_f + (k_f - k_s)\varphi} \tag{9}$$

This model has been previously used by Kefayati et al. [11], Xuan and Roetzel [10], Khanafer et al. [12] and many other authors. Note that the MG model is restricted to nanoparticles with the same spherical shape and suitable for small temperature gradients. The viscosity of the nanofluid can be approximated as viscosity of a base fluid lf containing dilute suspension of fine spherical particles and is given by Brinkman [16]:

$$\mu_{nf} = \frac{\mu_f}{(1-\varphi)^{2.5}} \tag{10}$$

All terms are defined in the Nomenclature.

The following dimensionless variables for natural convection are defined based on properties of pure fluid:

$$x = \frac{\tilde{x}}{L}\ ;\ y = \frac{\tilde{y}}{L}\ ;\ \omega = \frac{\tilde{\omega}L^2}{\alpha_f}\ ;\ \psi = \frac{\tilde{\psi}}{\alpha_f}\ ;\ \theta = \frac{T - T_c}{T_h - T_c}\ ;\ t = \frac{\tilde{t}\alpha_f}{L^2} \tag{11}$$

Dimensionless numbers for the system are defined as:

$$Ra = \frac{g\beta_f (T_h - T_c)L^3}{\alpha_f \nu_f},\quad Pr = \frac{\nu_f}{\alpha_f} \tag{12}$$

By using the dimensionless parameters, the equations are written as:

$$\frac{\partial^2\psi}{\partial x^2} + \frac{\partial^2\psi}{\partial y^2} = -\omega \tag{13}$$

$$\frac{\partial\omega}{\partial t} + \frac{\partial\psi}{\partial y}\left(\frac{\partial\omega}{\partial x}\right) - \frac{\partial\psi}{\partial x}\left(\frac{\partial\omega}{\partial y}\right) = A\,.Pr\left(\frac{\partial^2\omega}{\partial x^2} + \frac{\partial^2\omega}{\partial y^2}\right) + B.Pr.Ra\frac{\partial\theta}{\partial x} \tag{14}$$

$$\frac{\partial\theta}{\partial t} + \frac{\partial\psi}{\partial y}\left(\frac{\partial\theta}{\partial x}\right) - \frac{\partial\psi}{\partial x}\left(\frac{\partial\theta}{\partial y}\right) = \lambda\left(\frac{\partial^2\theta}{\partial x^2} + \frac{\partial^2\theta}{\partial x^2}\right) \tag{15}$$

Where A , B , and λ are given by the following relations:

$$A = \frac{1}{(1-\varphi)^{2.5}\left((1-\varphi) + \varphi\frac{\rho_s}{\rho_f}\right)}$$
$$B = \frac{1}{\frac{(1-\varphi)}{\varphi}\frac{\rho_f}{\rho_s} + 1}\frac{\beta_s}{\beta_f} + \frac{1}{\frac{\varphi}{1-\varphi}\frac{\rho_s}{\rho_f} + 1} \tag{16}$$
$$\lambda = \frac{(k_{nf})/(k_f)}{(1-\varphi) + \varphi\frac{(\rho C_p)_s}{(\rho C_p)_f}}$$

The dimensionless horizontal and vertical velocities can be written as:

$$u = \frac{\partial \psi}{\partial y}, \quad v = -\frac{\partial \psi}{\partial x} \tag{17}$$

The dimensionless boundary conditions are written as:

$$\begin{aligned}
&\theta = 0,\ u = v = \psi = 0,\ \omega = -\partial^2\psi/\partial x^2 && \text{on right wall of the enclosure}\\
&\theta = 1,\ u = v = \psi = 0,\ \omega = -\partial^2\psi/\partial x^2 && \text{on left wall of the enclosure}\\
&\partial\theta/\partial y = 0,\ u = v = \psi = 0,\ \omega = -\partial^2\psi/\partial y^2 && \text{on top and bottom walls of the enclosure}\\
&\theta = 0,\ u = v = \psi = 0 && \text{on the cold block}
\end{aligned} \tag{18}$$

The total mean Nusselt number of all walls of the enclosure and the block is defined as:

$$\overline{Nu}_{tot} = \frac{1}{L}\int_0^L \frac{k_{nf}(\varphi)}{k}\left\{\left|\frac{\partial\theta}{\partial x}\right|_{left} + \left|\frac{\partial\theta}{\partial x}\right|_{right}\right\}dy + \frac{1}{h}\int_0^h \frac{k_{nf}(\varphi)}{k}\left\{\left|\frac{\partial\theta}{\partial x}\right|_{left} + \left|\frac{\partial\theta}{\partial x}\right|_{right}\right\}dy + \frac{1}{w}\int_{\frac{L}{2}-\frac{w}{2}}^{\frac{L}{2}+\frac{w}{2}} \frac{k_{nf}(\varphi)}{k}\left|\frac{\partial\theta}{\partial y}\right|_{upper} dx \tag{19}$$

4 NUMERICAL DETAILS

The discretization procedure of the governing equations (Eqs. (13)–(15)) and boundary conditions described by Eq. (18) were solved numerically using an implicit stable finite difference technique. The vorticity and energy equations are solved using the ADI (Alternating Direction Implicit) method and the stream function equation is solved by the SLOR (Successive Line Over Relaxation) method while upwind difference is used for convective terms for the sake of numerical stability. Line by line application of TDMA (Tri-Diagonal Matrix Algorithm) method [17] is applied on the vorticity and energy equations until sum of the residuals became less than 10^{-6}. The developed algorithm was implemented in FORTRAN program.

4.1 GRID INDEPENDENCE STUDY

In order to determine a proper grid for the numerical simulation, a square enclosure filled with Cu–water nanofluid $(\varphi = 0.1)$ having a cold block with height and width respectively $w = 0.25L$ and $h = 0.5L$ is analyzed in two extreme Rayleigh numbers ($Ra = 10^4$ and 10^6). The mean Nusselt number obtained using different grid numbers for particular cases is presented in Table 2. As can be observed from the table, a uniform 103×103 grid is sufficiently fine for the numerical calculation.

Table 2. Effect of the grid size on $\overline{Nu}_{tot}$ for the cavity filled with the Cu–water nanofluid $(\varphi = 0.1)$ having a cold block with height and width respectively $w = 0.25L$ and $h = 0.5L$

Ra	63×63	83×83	103×103	123×123
10^4	11.261	11.243	11.235	11.231
10^6	22.173	22.165	22.161	22.159

4.2 VALIDATIONS

The present numerical scheme was validated against various numerical results available in the literature. the benchmark problem of natural convection in a square cavity which considered by De Vahl Davis [1] filled with Air $(Pr = 0.71)$. Table 3 demonstrates an excellent comparison of the average Nusselt number between the present results and the numerical results found in the literature [13-14]. Fig. 2 illustrates a comparison of the isotherms and streamlines between the present results and the results reported by Brakos et al. [13] at different Rayleigh number.

Table 3. Comparison of $\overline{Nu}$ between the present results and those reported in the literature for a DHC at different Rayleigh numbers

Ra	10^3	10^4	10^5	10^6
de Vahl Davis [1]	1.118	2.243	4.519	8.799
Relative Error (%)	0.26	0.44	3.2	0.73
Barakos and Mitsoulis [13]	1.114	2.245	4.510	8.806
Relative Error (%)	0.62	0.35	3.2	0.65
Dixit and Babu [14]	1.118	2.256	4.519	8.817
Relative Error (%)	0.26	0.13	4.8	0.75
Present study	1.121	2.253	4.673	8.864
Grid size	83^2	83^2	103^2	103^2

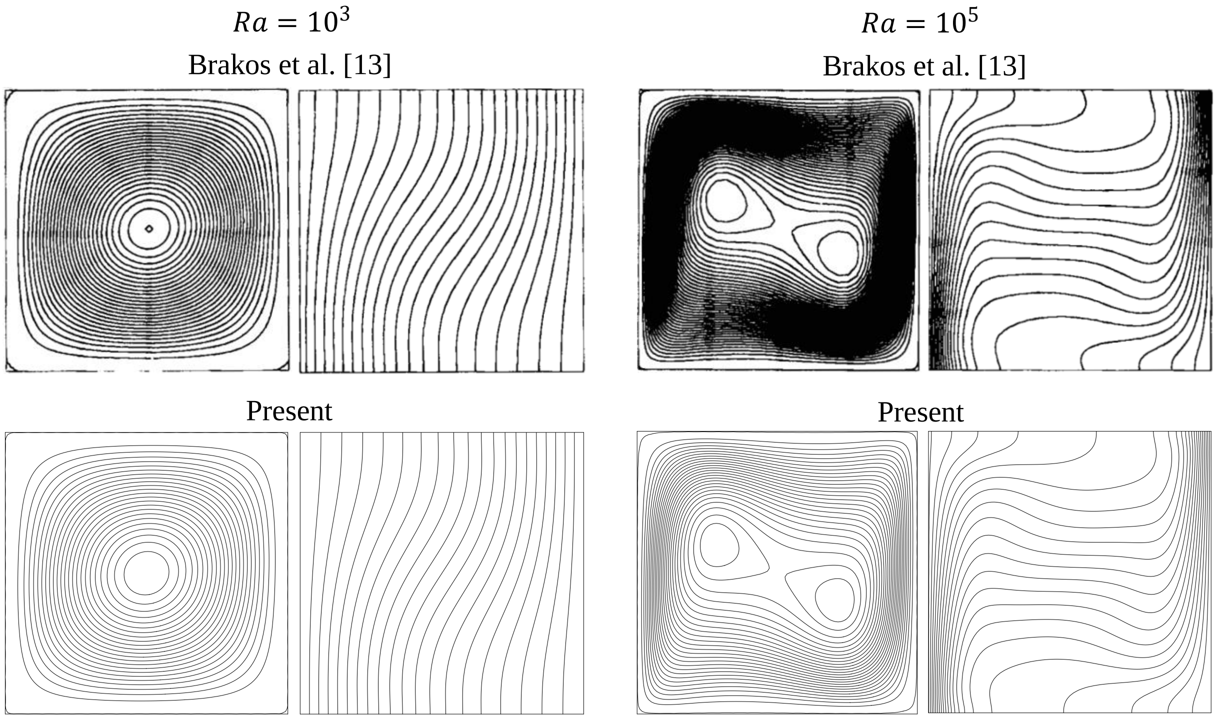

Fig. 2. Comparison of the streamlines and isotherms between the present results and that of Brakos et al. [13] at various Rayleigh numbers

5 RESULTS AND DISCUSSION

In the present study, numerical results of natural convection fluid flow and heat transfer of Cu-water nanofluid inside a square enclosure with a cold block are investigated. The results are generated for different pertinent dimensionless groups: the height of the obstacle $(0.125 \leq H \leq 0.5)$, Rayleigh number $(10^3 \leq Ra \leq 10^6)$, and nanoparticles volume fraction $(0 \leq \varphi \leq 0.2)$, while the width of the block w is fixed at $0.25L$ and the Prandtl number of the pure water $(Pr = 6.2)$.

Fig. 3 displays effects of cooler dimensionless height on the streamlines and isotherms when $Ra = 10^4$. We can see in Fig. 3(a) that the flow structure is organized into one convection cell on right side of the enclosure. isotherms shown in Fig. 3(b) are uniformly distributed which indicate that the heat transfer in the enclosure was governed mainly by the conduction mode. By increasing cooler height from $H = 0.25$ to $H = 0.5$, the central core of the convection cell changes significantly. By increasing Rayleigh number from 10^4 to 10^6, it was observed in Fig. 4(b) that the patterns of isotherms became complex which means that the heat transfer mechanism is changing from conduction to the convection. By increasing the cooler dimensionless height, we can see clearly in Fig. 4(a) that the rotating eddy became with two inner vortices due to the stronger convection effects.

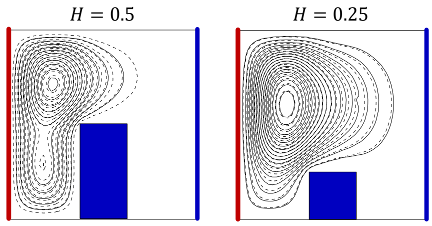

(a) streamlines

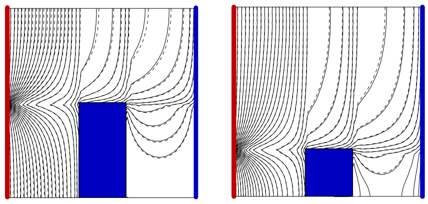

(b) isotherms

Fig. 3. ***Effect of varying cooler height on (a) the streamlines and (b) isotherms*** $(Ra = 10^4,\ W = 0.25)$ ***with case of pure fluid (dashed line) and Cu-water (solid line) nanofluid with*** $\varphi = 0.1$

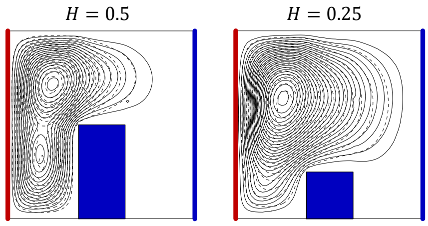

(a) streamlines

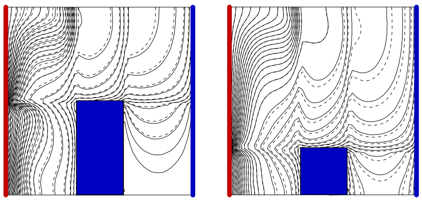

(b) isotherms

Fig. 4. ***Effect of varying cooler height on (a) the streamlines and (b) isotherms*** $(Ra = 10^6,\ W = 0.25)$ ***with case of pure fluid (dashed line) and Cu-water (solid line) nanofluid with*** $\varphi = 0.1$

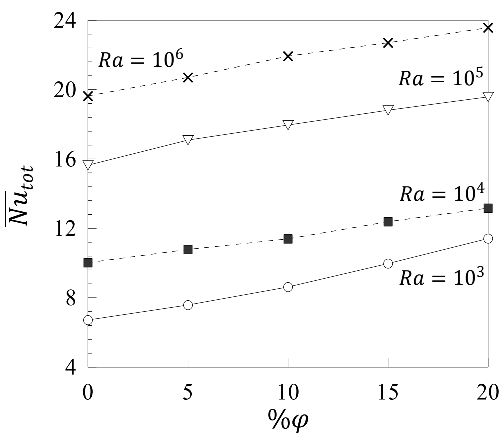

Fig. 5. ***Variation of*** $\overline{Nu}_{tot}$ ***for different Rayleigh numbers and volume fraction of the nanoparticles*** $(H = 0.5)$

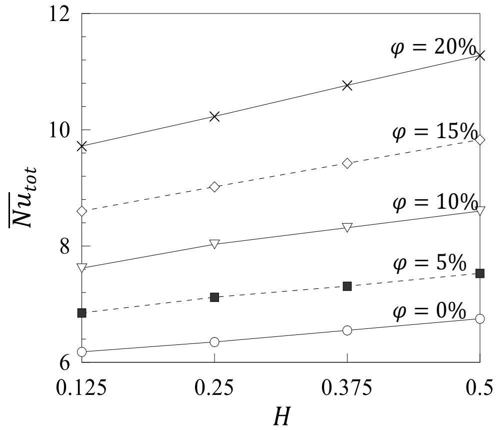

Fig. 6. ***Effect of the cooler height on $\overline{Nu}_{tot}$ for different volume fraction of the nanoparticles*** $(Ra = 10^3)$

The effect of the concentration of nanoparticles on $\overline{Nu}_{tot}$ is illustrated in Fig. 5 for various Ra in the case of the cooler height $H = 0.5$. It is seen that the heat transfer is always improved by increasing volume fraction of the nanoparticles, but the rate of improvement depends on Ra. By increasing Rayleigh number, the heat transfer rate increases. We can see also from the curves of Fig. 5 that $\overline{Nu}_{tot}$ displays a quasi-linear variation with the parameter φ. This quasi-linearity was also remarked for the other cooler heights (not presented here).

Fig. 6 shows the effect of the cooler height on $\overline{Nu}_{tot}$ for different volume fraction of the nanoparticles in the case of $Ra = 10^3$. This is evident in Fig. 6 as the height of the cooler increases; the total mean Nusselt number $(\overline{Nu}_{tot})$ is augmented due to additional surface area offered by the cooler for heat transfer communication.

6 Heat Transfer Correlation

The total mean Nusselt number $(\overline{Nu}_{tot})$ is correlated over a wide range of design parameters employed in this investigation, such as the height of the obstacle $(0.125 \leq H \leq 0.5)$, Rayleigh number $(10^3 \leq Ra \leq 10^6)$, and nanoparticles volume fraction $(0 \leq \varphi \leq 0.2)$, These correlations can be mathematically expressed as follows:

$$\overline{Nu}_{tot} = 20.803\ \varphi + 2.178\ Ra^{0.161}$$

Where H is fixed at 0.5 and the confidence coefficient for the above equation is $R^2 = 98.6\%$.

$$\overline{Nu}_{tot} = (1.482 + 6.676\ \varphi + 34.367\ \varphi^2)H + 15.963\ \varphi + 5.873$$

Where Ra is fixed at 1000 and the confidence coefficient for the above equation is $R^2 = 99.1\%$.

7 Conclusion

Natural convection heat transfer of nanofluid (Cu-water) in a square enclosure having a cold obstacle. was studied numerically for various design parameters such as the height of the obstacle (H), Rayleigh number (Ra) and nanoparticles volume fraction (φ). According to the presented results, the following conclusions are drawn:

- In the wide range of design parameters, the heat transfer is improved by increasing both the Rayleigh number (Ra) and the nanoparticle volume fraction(φ).
- The height of the cooler has significant effect on flow, temperature fields, and heat transfer
- By increasing the height of the cooler the total mean Nusselt number $(\overline{Nu}_{tot})$ is augmented due to additional surface area offered by the cooler for heat transfer communication.
- The total mean Nusselt number displays a quasi-linear variation with the parameter φ and H .
- The heat transfer correlations show that, the height of the obstacle, Rayleigh number and nanoparticles volume fraction increased the total mean Nusselt number.

NOMENCLATURE

C_p	specific heat, $Jkg^{-1}K^{-1}$
g	gravitational acceleration, $m\ s^{-2}$
h	height of the cold block, m
H	non-dimensional height of the cold
k	thermal conductivity, $W\ m^{-1}K^{-1}$
L	enclosure height, m
$\overline{Nu}_{tot}$	total mean Nusselt number, defined in Eq. (19)
Pr	Prandtl number $\left(= \nu_f/\alpha_f\right)$
Ra	Rayleigh number $\left(= g\beta_f(T_h - T_c)L^3/\alpha_f\nu_f\right)$
T	temperature, K
$\tilde{t}$	time, s
t	dimensionless time $(\tilde{t}\alpha_f/L^2)$
$\tilde{u}, \tilde{v}$	velocity components, ms^{-1}
u, v	dimensionless velocity components
w	dimensional width of the cold block
W	dimensionless width of the cold block
$\tilde{x}, \tilde{y}$	Cartesian coordinates, m
x, y	dimensionless Cartesian coordinates

Greek symbols

β	thermal expansion coefficient, K^{-1}
θ	dimensionless temperature
μ	dynamic viscosity, $kg\ m^{-1}s^{-1}$
ν	kinematic viscosity, m^2s^{-1}
ρ	density,kgm^{-3}
φ	volume fraction of the nanoparticles
$\tilde{\psi}$	dimensional stream function m^2s^{-1}
ψ	dimensionless stream function
$\tilde{\omega}$	dimensionless vorticity
ω	dimensional vorticity (s^{-1})

Subscripts

c	cold
f	fluid
h	hot
nf	nanofluid
s	solid nanoparticles

REFERENCES

[1] G. De Vahl Davis, Natural convection of air in a square cavity: a bench mark numerical solution, Int. J. Numer. Methods Fluids 3 (1983) 249–264.

[2] A. AlAmiri, K. Khanafer, and I. Pop, “Buoyancy-induced flow and heat transfer in a partially divided square enclosure,” International Journal of Heat and Mass Transfer, vol. 52, no. 15-16, pp. 3818–3828, 2009.

[3] J. Guiet, M. Reggio, P. Vasseur, Natural Convection of Nanofluids in a Square Enclosure with a Protruding Heater, Advances in Mechanical Engineering (2012). article ID 167296.

[4] Y. Varol, H. F. Oztop, and T. Yilmaz, “Natural convection in triangular enclosures with protruding isothermal heater,” International Journal of Heat and Mass Transfer, vol. 50, no. 13-14, pp. 2451–2462, 2007.

[5] Z. Boulahia and R. Sehaqui, “Numerical Simulation of Natural Convection of Nanofluid in a Square Cavity Including a Square Heater,” International journal of science and research (IJSR), vol.4, issue 12, p. 1718-1722, 2015.

[6] Bouafia M., Daude O., Natural convection for large temperature gradients around a square solid body within a rectangular cavity, Int. J. Heat Mass Transfer, 50, 3599-3615, 2007.

[7] Yeong Ha M, Mi J J., A numerical study on three-dimensional conjugate heat transfer of natural convection and conduction in a differentially heated cubic enclosure with a heat-generating cubic conducting body, Int. J. Heat Mass Transfer, 43, 4229-4248, 2000.

[8] F. Garoosi, G. Bagheri, F. Talebi, Numerical simulation of natural convection of nanofluids in a square cavity with several pairs of heaters and coolers (HACs) inside, Int. J. Heat Mass Transfer 67 (2013) 362– 376.

[9] M. El Abdallaoui, M. Hasnaoui and A. Amahmid, Numerical simulation of natural convection between a decentered triangular heating cylinder and a square outer cylinder filled with a pure fluid or a nanofluid using the lattice Boltzmann method, Powder Technol. 277 (2015) 193–205

[10] Y. Xuan, W. Roetzel, Conceptions for heat transfer correlation of nanofluids, Int. J. Heat Mass Transf. 43 (2000) 3701–3707.

[11] G.H.R. Kefayati, Lattice Boltzmann simulation of MHD natural convection in a nanofluid-filled cavity with sinusoidal temperature distribution, Powder Technol. 243 (2013) 171–183.

[12] K. Khanafer, K. Vafai, M. Lightstone, Buoyancy-driven heat transfer enhancement in a two-dimensional enclosure utilizing nanofluids, Int. J. Heat Mass Transf. 46 (2003) 3639–3653.

[13] G. Barakos, E. Mitsoulis, Natural convection flow in a square cavity revisited: laminar and turbulent models with wall functions, Int. J. Numer. Methods Fluids 18 (1994) 695–719.

[14] H.N. Dixit, V. Babu, Simulation of high Rayleigh number natural convection in a square cavity using the lattice Boltzmann method, Int. J. Heat Mass Transfer 49 (2006) 727–739.

[15] Maxwell, J.C., “A Treatise on Electricity and Magnetism”, Clarendon Press, U.K, (1891).

[16] Brinkman, H.C., 1952. The viscosity of concentrated suspensions and solutions. J. Chem. Phys. 20, 571–581.

[17] S.V. Patankar, Numerical Heat Transfer and Fluid Flow, McGraw-Hill, Washington, 1980.